

# Influence of steel-fiber type and content on electrical resistivity of old-concrete

Tayfun Uygunoğlu<sup>\*1</sup>, İlker Bekir Topçu<sup>2</sup> and Barış Şimşek<sup>3</sup>

<sup>1</sup>Engineering Faculty, Civil Engineering Department, Afyon Kocatepe University, 03200, Afyonkarahisar, Turkey

<sup>2</sup>Engineering-Architectural Faculty, Civil Engineering Department, Eskişehir Osmangazi University, 26480, Eskişehir, Turkey

<sup>3</sup>Faculty of Engineering, Department of Chemical Engineering, Çankırı Karatekin University, 18120 Çankırı, Turkey

(Received January 24, 2017, Revised September 6, 2017, Accepted September 10, 2017)

**Abstract.** Electrical resistivity is a property associated with both the physical and chemical characteristics of concrete. It allows the evaluation of the greater or lesser difficulty with which aggressive substances penetrate the concrete's core before the dissolution of the passive film process and the consequent reinforcement's corrosion begin. This work addresses the steel fiber addition to concrete with two types and various contents from 0% to 1.3%, correlating it with its electrical resistivity. To that effect, 9 different mixes of steel fiber reinforced concrete (SFRC) were produced. The electrical resistivity was evaluated on the on six years aged SFRC by direct measurement at different frequency from 0.1 kHz to 100 kHz. The results indicate that steel fiber content is strongly conditioned by the type and quantity of the additions used. It was also found that long type of fibers has more effect on decreasing the electrical resistivity of concrete than short fibers. Therefore, they increase the corrosion risk of concrete depending on fiber volume fraction and moisture percentage.

**Keywords:** steel fiber; old-concrete; electrical resistivity; carbonation

## 1. Introduction

Deterioration of concrete composite structures is inevitable due to the fact that it is subjected to harsh environmental factors. Therefore, inspection and maintenance of these structures should be done to ensure their serviceability. Moreover, structures vary in construction methods, structural design, construction materials, concrete mixes and quality control in place for construction process and inspection and so on (Perumal 2014, Salbei *et al.* 2014). The on-site monitoring of materials and elements represents an important issue since it is mandatory in order to provide a complete structural and mechanical evaluation of the construction. In this case, the critical aspect is to assess information about the materials by means of a nondestructive (NDT) analysis. This requires performing the in situ analysis, by having access only to the surface of the element to be monitored (Faifer 2011).

Electrical resistivity measurement among the NDT techniques is becoming popular among researchers for the quality control and durability assessment of concrete. Durability of concrete depends largely on the as pore size distribution and the shape of the pore interconnections. A finer pore network, with less connectivity, leads to lower permeability. A porous microstructure with larger degree of interconnections, on the other hand, results in higher permeability and reduced durability in general. Electrical response of cementitious systems can be used to understand the evolving microstructure, and thus to provide indications of the mechanical and durability performance of such

systems (Neithalath *et al.* 2010). Electrical measurements on cement-based materials using direct current (DC), (Wen *et al.* 2000) or alternating current (AC), (Gu *et al.* 2000, Peled *et al.* 2001) have been utilized to detect and quantify cracking and damage. Overall, the electrical resistivity of concrete can be described as the ability of concrete to withstand the transfer of ions subjected to an electrical field. In general performing electrical measurements directly on cement-based materials is limited to small geometries due to the large impedance of concrete materials (Halaji and Ghaz 2014). Experience obtained from existing structures suggests that the current codes and practice do not provide a sufficiently controlled durability, and performance based methods should be used (Gjørsv 2013).

Electrical resistance and its durability indicator counterpart, electrical resistivity, are parameters that are commonly related to transport properties of concrete (Pacheco *et al.* 2014). Measured values are usually between  $10^1$  to  $10^5$  ohm, which are dependent on concrete composition, cement type, age and environmental conditions (Polder *et al.* 2000, Bertolini *et al.* 2004). Faifer *et al.* (2011) used a new method to the estimation of the fiber density and their average orientation by the employment of a probe that is sensitive to the magnetic properties of the steel fibers. The developed measurement system and the collected measurements showed a good agreement between the expected and the experimental results. Kyung *et al.* (2007) investigated the measurement of potentials in concrete by analytically. The effect of internal defects on the potentials measured is clarified numerically by the boundary element method (BEM). A simplified inversion by boundary element method was applied to convert the potentials on concrete surface to those on rebars, taking into account the concrete resistivity. Xiao *et al.*

\*Corresponding author, Professor  
E-mail: [uygunoglu@aku.edu.tr](mailto:uygunoglu@aku.edu.tr)

Table 1 Classification of corrosion versus resistivity of concrete

Concrete resistivity, kΩ.m	Corrosion risk
<0.1	High
0.1-0.5	Moderate
0.5-1.0	Low
>1.0	Negligible

(2008) used electrical resistivity for measurement and Marsh cone for provide a quick way to evaluate and select suitable superplasticizer in concrete. Koleva *et al.* (2008) researched the favorable effects of pulse cathodic protection current flow on the concrete matrix, which were additionally explained by microstructural analysis of the specimens. They found out that physicochemical changes due to ion transport as well as electrical properties of the concrete matrix were attributed to the structural alterations of the pore space induced by the cathodic protection current. Neithalath *et al.* (2010) used a methodology utilizing a generalized effective media theory to predict the pore volume fraction and the strength of hydrating cementitious materials in their research. They considered that the evolving microstructure was also related to a maturity index. Yury *et al.* (2014) studied a contact method to measure the resistivity of unsaturated concrete samples. As a result of their study, resistivity is related to the volumetric fraction of conducting water in pores and its hygroscopic equilibrium with the surrounding environment. Monteiro *et al.* (2015) researched electrical properties of cement-based composites doped with carbon black nanoparticles (CB). According to the results of their study, a decrease in resistivity occurs, which has been followed by an increase of the stress sensitivity when rising the CB amount in the mixture. Polder (2001) researched relationship between corrosion rate and resistivity. As a result, a classification was reported depending on electrical resistivity and corrosion risk for reinforced concretes (Table 1). Moris *et al.* (2002) also reported that there are good relation between corrosion and electrical current.

While the measurement of electrical resistance of concrete looks very simple at first glance, the complex microstructure of concrete makes it difficult to find a reliable technique. The inherent electrical resistivity of concrete is affected by the pore size distribution and interconnection, conductivity of pore fluid, degree of saturation, concrete component and temperature. On the other hand, as a part of the reinforcement corrosion circuit, the resistivity of concrete is a decisive material parameter with regard to corrosion propagation, which itself is a time-dependent process of many years of length. For this reason, a picture of the long term behavior of the resistivity of concrete could be of great value. Steel fibers have been known as special applications of structural concrete for decades and the use of steel fiber reinforced concrete (SFRC) has gradually increased in recent years. Steel fibers are nowadays also used in combination with traditional reinforcement for structural concrete, where the role of the fibers is to minimize the crack widths, shrinkage and/or increase the mechanical loading whereas the traditional

Table 2 Characteristics of OPC

Chemical properties	%
CaO	62.17
SiO <sub>2</sub>	20.02
Al <sub>2</sub> O <sub>3</sub>	4.36
Fe <sub>2</sub> O <sub>3</sub>	3.79
MgO	0.89
SO <sub>3</sub>	2.86
K <sub>2</sub> O	0.8
Na <sub>2</sub> O	0.13
Cl <sub>-</sub>	0.01
Insoluble residue	0.56
LOI	1.78
Components (Bogue) %	
C <sub>3</sub> S	58.07
C <sub>2</sub> S	13.77
C <sub>3</sub> A	5.14
C <sub>4</sub> AF	11.53

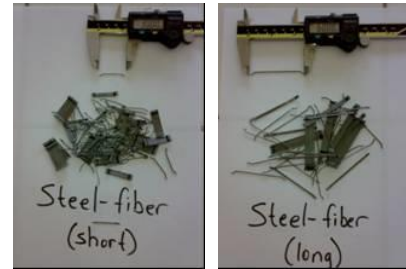


Fig. 1 Steel fibers used in the experiments

reinforcement bars are used for structural purpose (Solgaard *et al.* 2013). There are some articles have been published on various aspects of corrosion assessment with electrical measurement of long term hardened concrete containing the steel fibers. Therefore, this paper aimed to study the electrical resistivity of concrete to which steel fiber was added on various amounts from 0% to 1.3%. In view of these observations, the objective of the present research is to introduce NDT techniques for corrosion assessment, because rebar corrosion due to carbonation and chloride ingress is found to be the dominant cause of deterioration in most concrete structures worldwide.

## 2. Experimental program

### 2.1 Materials used

Ordinary Portland cement (OPC) was used in the experiments with a minimum strength of 45 MPa at 28 days (CEM I 42.5 R). It complies with the requirement of European Standards EN 197-1. Characteristic properties of cement are given in Table 2. The maximum 22 mm nominal size of crushed aggregate was used. The coarse aggregates were calcareous stone as crushed stone I (CS I) in 6-12 mm; and crushed stone II (CS II) in 12-22 mm. Their specific gravity is 2.70 and 2.71, respectively. The fine aggregates were natural sand (NS), with specific gravity of 2.58, in 0-3

Table 3 Mixture proportions of SFRC for per cubic meter

Components	Contents, kg/m <sup>3</sup>								
	Control	LF-60 type fiber				SF-30 type fiber			
		25	50	75	100	25	50	75	100
Cement	350	352	351	351	352	352	353	354	354
Water	210	211	211	211	211	211	212	212	213
NS	341	341	339	337	336	341	341	340	338
CSS	340	340	337	336	335	340	339	339	337
CS I	539	539	535	534	533	540	539	538	536
CS II	537	537	533	532	531	538	537	536	534
Steel fiber	-	25	50	75	101	25	50	76	101
Admixture	35	35	35	35	35	35	35	35	35
Air (%)	1.3	1.2	1.8	2.0	1.97	1.06	1.1	1.2	1.4

mm and crushed stone sand (CSS), with specific gravity of 2.57, in 0-6 mm. Fibers, added to concrete, were in two different types (Fig. 1). They were made with drawn low-carbon steel and hooked-end type. Modulus of elasticity of steel fibers is 200 MPa. The fiber lengths ( $l$ ) were 60 mm and 30 mm, the diameters ( $d$ ) were 0.75 mm and 0.5 mm; therefore, the aspect ratios ( $l/d$ ) were 80 and 60, respectively, for long (LF) and short (SF) fibers. These fibers are available in bundles of about 30 fibers, which were separated with water-soluble glue to ensure immediate dispersion in concrete during mixing. Polycarboxylic based new generation superplasticizer admixture was also used to obtain a good workability for fresh SFRC mixture.

## 2.2 Concrete mixes

Cement dosage, water to cement ratio and chemical admixture content were 350 kg/m<sup>3</sup>, 0.6 lt/kg and 1.0% (by weight of cement), respectively, in the mixtures. The volume of aggregate was determined for reference Portland cement concrete by assuming approximately 1.5% air is trapped in fresh concrete. The volume of aggregate was used to determine the aggregate weight. The strength of the bond between particles and full coating of cement binder to the aggregate and fiber increases by encouraged proper mixing. The mixing of concrete batches was carried out, using a small drum mixer. The concrete dried components were mixed during 2 min. Then, to encourage a uniform distribution of fibers throughout of the concrete, fibers were added to the concrete mix by slowly and evenly after the water (with diluted admixture), aggregates and cement have been fully mixed. The fresh concrete was mixed for 3 min and was poured to moulds in size of 100×100×150 mm. The mix material is required to be in uniform distributed and consistency in the concrete mix. The nine different series were designed by using two fiber types and fiber contents as 0 (control) kg/m<sup>3</sup>, 25 kg/m<sup>3</sup>, 50 kg/m<sup>3</sup>, 75 kg/m<sup>3</sup> and 100 kg/m<sup>3</sup>. Using the total volume of each type of fibers, the weight of each type of fiber was obtained by specific gravity. Specific gravity of each type of fibers was 7.8 kg/m<sup>3</sup>. Therefore, volume fractions ( $V_f$ ) were 0% (control), 0.3%, 0.64%, 0.1% and 1.3% of volume of concrete. Mixture proportion for per cubic meter of SFRC was given in Table 3. For more information about SFRC i.e., fresh and

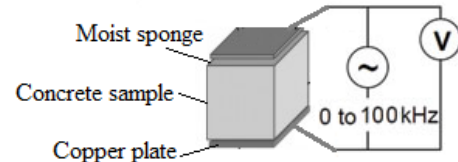


Fig. 2 Electrical resistivity measurement on SFRC

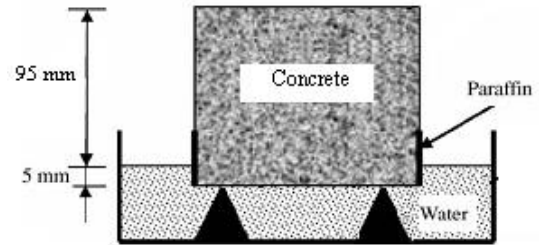


Fig. 3 Schematic presentation of capillary sorptivity setup

hardened strength properties please see reference (Uygunoglu 2010).

## 2.3 Electrical resistivity of concrete

The test aimed to determine the differences in electrical resistivity measured at different types of steel fiber and different amounts of steel fiber changing from 0 to 1.3%, which were added to concrete. To that effect, 9 different mixes of steel fiber reinforced concrete (SFRC) were used. The SFRC samples cured at lime saturated water at 20±2°C for 28 days, and they were cured at inside of laboratory (65% of humidity) for 6 months, and then they were waited at outside of laboratory (atmospheric condition) for 5.5 years. The electrical resistivity was evaluated by direct measurement (two-point uniaxial) under AC with frequency of 100 Hz, 120 Hz, 1 kHz, 10 kHz and 100 kHz, on the six years aged SFRC specimens by LCR meter according to ASTM C 1760 (2012) (Fig. 2).

The measurements were carried out on both oven dried and water saturated concretes. The concrete sample was placed between two electrodes (two parallel copper plates) with moist sponge contacts at the interfaces to ensure a proper electrical connection. The electrical resistivity ( $R$ ) of concrete was calculated by Eq. (2) as follows.

$$\rho = R \times \frac{A}{l} \quad (2)$$

where,  $\rho$  is resistivity ( $\Omega\cdot m$ ),  $R$  is resistance ( $\Omega$ ),  $A$  is sample area (cm<sup>2</sup>) and  $l$  is sample length (m).

## 2.4 Capillary sorptivity and porosity

The apparent porosity of 6 years aged specimens was carried out according to Archimedes principle by the weight measurements of saturated specimens in air and in water, and dry weight (oven drying at 105°C to constant weight). A test to determine the capillarity coefficient of specimens was also determined by using specimens preconditioned and dried in an oven at about 105±5°C to the constant mass. As shown in Fig. 3, the test specimen was exposed to water

through a plane cross-section (100×100 mm) by placing it in a pan.

The water level in the pan was maintained at about 5 mm above the bottom of the specimen during this experiment. The surfaces of the specimen below the water level were coated with paraffin to achieve unidirectional flow. At regular times such as 1st, 4th, 9th, 16th, 25th and 36th minutes, the mass of the specimen was measured using a balance, then the amount of water adsorbed was calculated and normalized regarding the cross-section area of the specimen (Hanžič and Ilić 2003, Tasdemir 2003). Therefore, capillarity coefficient was obtained for each steel fiber contents in experimental study by Eq. (1), as follows

$$q = k\sqrt{t} \quad (1)$$

where  $k$  is capillarity coefficient ( $\text{cm}^2/\text{min}$ );  $q$  is water absorption quantity in cross-section of specimens ( $\text{cm}^3/\text{cm}^2$ ); and  $t$  is time (min).

### 2.5 Carbonation depth

An accelerated carbonation test was carried out according to the phenolphthalein test for measuring carbonation depth was determined by RILEM CPC-18 (1998). Phenolphthalein solution is prepared as a 1% solution in 70% ethyl alcohol was sprayed onto the concrete surface which has been cleaned of dust and loose particles. Phenolphthalein is a colorless acid indicator which turns red when the pH is above a value of 9.5, that is, when the concrete is alkaline. If no coloration occurs, carbonation has taken place and the depth of the carbonated surface layer can be measured.

## 3. Results and discussion

As a result of experiments, the concrete to which fiber was not added had the most electrical resistivity, which was given in Fig. 4(a)-(b) for dry condition. It was observed that when the fiber was added to specimens and its amount increased from 0.5% to 1.3%, electrical resistivity decreased regardless of frequency. When the specimens with LF were compared with the specimens with SF, it was seen that the electrical resistivity had the lowest value at the specimens with LF. It was thought that the reason why the concrete with short fibers had much more resistivity than the concrete with long fibers was long fibers' easing the current passage through much more contact with each other concrete.

The general representation of the electrical resistivity consists of low and high frequency ranges were also given in Fig. 4 and Fig. 5. The resistivity measurements were carried out at the frequency range of 0.1 to 100 kHz to obtain a relatively good representation of the real resistance of concrete. The use of a low frequency signal increased the measured resistivity compared to high frequency signal. While the characteristics of resistivity at higher frequencies are attributed to the microstructure of concrete, the characteristics in low frequency region are primarily influenced by conditions at the electrode-concrete interface. However, there is no general statement on the optimum

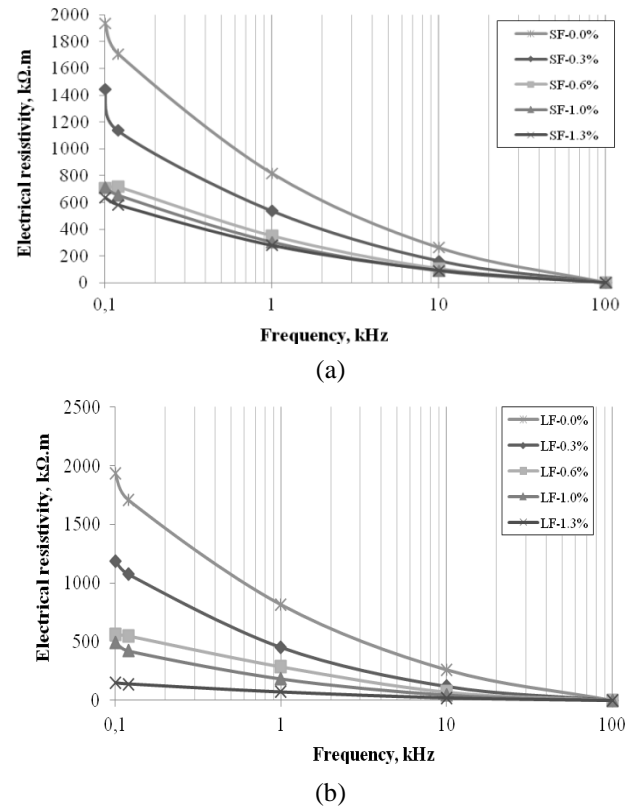


Fig. 4 Electrical resistivity of dried SFRC (a) small fiber; (b) long fiber

frequency, as it varies with mixture proportions and moisture conditions. The electrical resistivity significantly decreased with an increase of the frequency from 0.1 to 100 kHz for all fiber contents.

A change in the degree of saturation will affect the resistivity (or conductivity) of concrete as it would vary the amount of fluid in pore network. It is advisable to use a consistent curing method and ensure that the test specimens are in saturated surface dry condition at the time of testing to make reliable and repeatable electrical resistivity measurements for quality control applications. Concrete is a porous material, and it may exhibit conductive or insulating characteristics depending on the moisture content or the degree of the saturation of the pores. For example, a concrete sample might exhibit very high electrical resistance when it is dry, but the same concrete would have much lower resistance in a saturated condition. Fig. 5(a) and (b) show that moisture condition of SFRC affected the electrical resistivity of concrete substantially. As seen from Fig. 5, the moisture content has a predominant effect on the electrical resistivity of the composite. In saturated state, the concrete had approximately thousand times lower resistivity than that in dry condition at six years aged. Since the electrical current is carried by ions flowing through the pore solution in concrete, higher moisture content causes easier electrical flow and hence, the electrical resistivity decreases in saturated state (Şengül 2014). The reduced moisture content increases the electrical resistivity significantly. Therefore, it is very important to ensure the same moisture condition in different mixtures for quality control purposes.

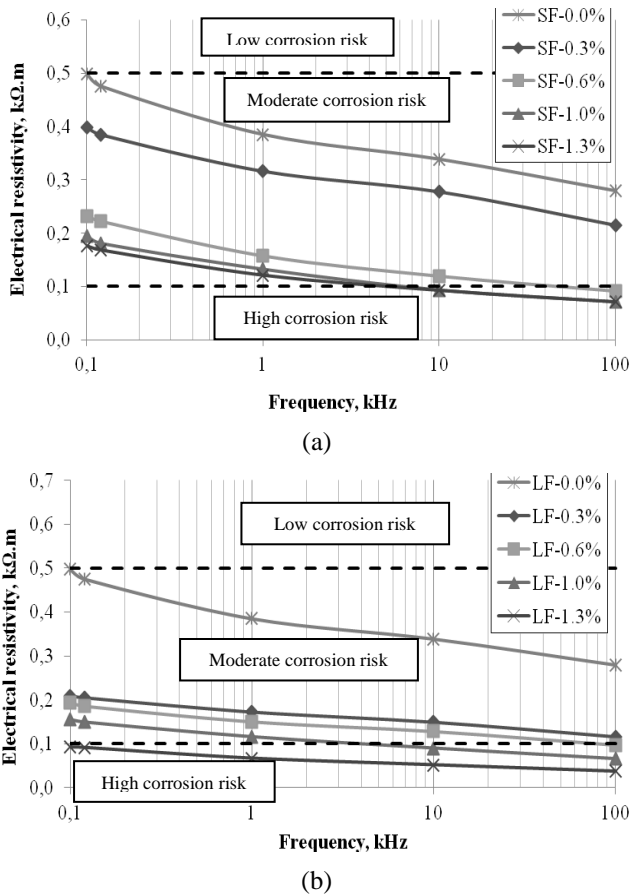


Fig. 5 Electrical resistivity of saturated SFRC (a) small fiber; (b) long fiber

The results of electrical resistivity measurements depending on fiber content for different conditions, are presented in Table 4 as equations. In Table 4, “y” defines the electrical resistivity when “x” is the fiber volume fraction. The correlations between the fiber volume fraction and electrical resistivity are very satisfactory, the lowest correlation coefficient is 0.86. Therefore, these equations can be used for determination of electrical resistivity of SFRC at different frequency measurement.

It is widely accepted that concrete resistivity can easily be measured, especially in the field, compared to other parameters such as the corrosion rate. The corrosion rate of steel can be examined indirectly by measuring the electrical resistivity of concrete. Currently, no standards exist that evaluate the corrosion resistance of SFRC. However, a relationship between concrete resistivity and corrosion rate would consequently allow the assessment of the corrosion stage in an efficient and reasonably priced way (Hornbostel 2013). As mentioned before, concretes conducting the electrical resistivity lower than 0.1 kΩ.m are regarded to undergo a high corrosion risk as embedded steels while the resistivity higher than 1.0 kΩ.m is regarded to passive corrosion risk (see Table 1). According to these limitations, corrosion was not observed at the concrete with and without fiber at dry conditions.

In order to detect the effect of moisture on the frequency dependence a series of SFRC specimens were tested at the

Table 4 Equations for electrical resistivity versus fiber content

	Dried concrete		Saturated concrete	
	Frequency, Hz	Equation	R	Equation
SF	100	$y=1764.7e^{-0.92x}$	0.93	$y=0.4833e^{-0.879x}$
	120	$y=1516.5e^{-0.849x}$	0.95	$y=0.4636e^{-0.889x}$
	1000	$y=725.24e^{-0.852x}$	0.96	$y=0.3766e^{-0.998x}$
	10000	$y=223.78e^{-0.85x}$	0.93	$y=0.3308e^{-1.154x}$
	100000	$y=1.7398e^{-1.534x}$	0.82	$y=0.2662e^{-1.203x}$
LF	100	$y=2074.7e^{-1.872x}$	0.97	$y=0.4077e^{-1.139x}$
	120	$y=1864.9e^{-1.855x}$	0.98	$y=0.3908e^{-1.123x}$
	1000	$y=851.08e^{-1.8x}$	0.99	$y=0.328e^{-1.212x}$
	10000	$y=243.02e^{-1.854x}$	0.99	$y=0.2928e^{-1.33x}$
	100000	$y=1.4698e^{-1.512x}$	0.86	$y=0.2392e^{-1.443x}$

same temperature conditions. Corrosion risk evaluation results are also given in Fig. 5(a) and (b) for saturated SFRC. By comparing the results with dried SFRC measurements, one can be clearly seen that moisture plays a profound role for the frequency dependence of measurements. It has been seen that when the frequency which is applied to the saturated specimens is increased, the risk of corrosion is generally increased. Furthermore, maximum corrosion has been observed at the specimens with long fibers to which AC current (frequency from 0.1 to 100 kHz) has been applied. When the fiber amount is more than 0.6% at the concrete with SF, the risk of high corrosion has been occurred at each frequency values from 0.1 kHz to 100 kHz. Moderate corrosion has been observed at the specimens without fibers for saturated conditions. However, high and very high corrosion risk was found on concrete with LF under frequency of 0.1 kHz to 100 kHz. The maximum corrosion risk was observed on concrete with LF content of up to 0.3% for all the frequency values. Accordingly, as being independent with the type of fiber, it can be interpreted that there will be high corrosion risk when fiber content of 1.0% or higher has been used in the concrete at saturated conditions. Investigations have found correlations between concrete resistivity and both the corrosion initiation and the propagation period. The corrosion often has an inverse correlation to the electrical resistivity of concrete (McCarter *et al.* 2010, Bouny *et al.* 2011). In general, higher electrical resistivity of concrete lowers the risk and the rate of corrosion (Michel *et al.* 2009).

The corrosion risk significantly depends on the different harmful materials and their accession into the concrete. The higher the concrete porosity is, the easier for these corrosive materials to get near to the embedded steel, consequently the durability of the structure becomes limited in time. The apparent porosity measurements of concrete can be carried out by analyzing the conductivity in a function of moisture content. Porosity and capillarity played paramount roles on electrical resistivity of concrete which is an indicator of durability. The porosity of SFRC versus steel fiber volume fraction is shown in Figure 6. It was observed that porosity increased with volume of steel fibers in concrete. With short fiber (SF) amount varied in the range of 0.0 to 1.3% by

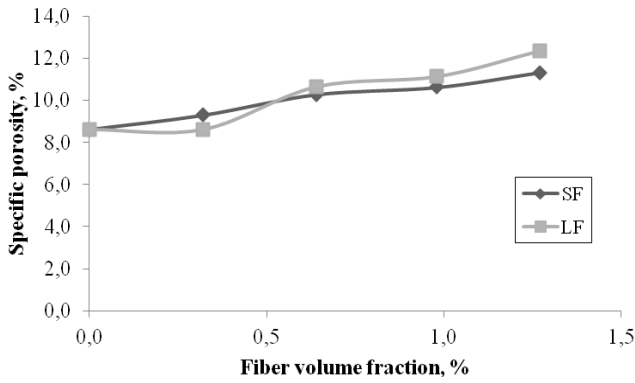
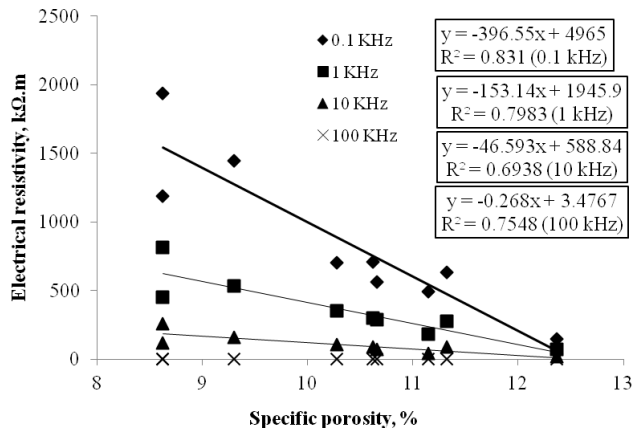
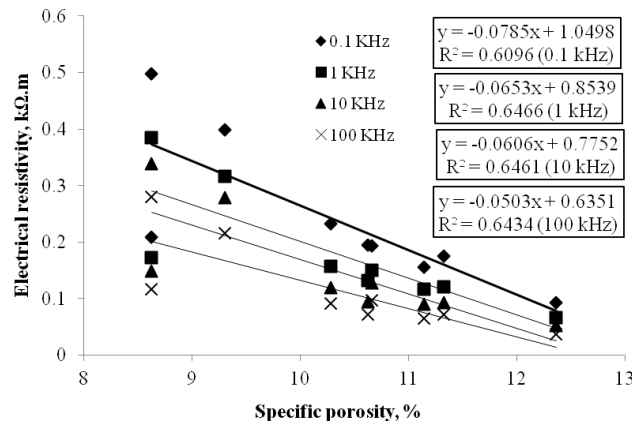


Fig. 6 Specific porosity of SFRC



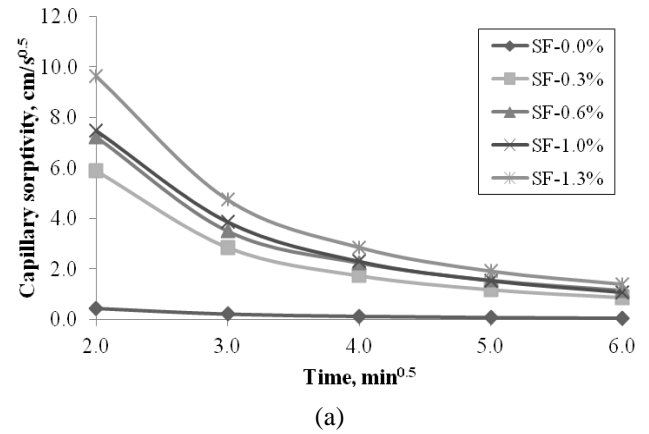
(a)



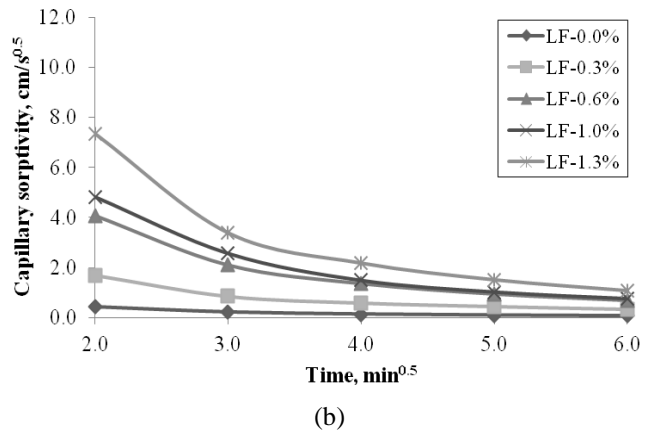
(b)

Fig. 7 Electrical resistivity of SFRC versus specific porosity (a) dried; (b) saturated

volume, the porosity varied from 8.6 to 11.3 %, as it can be seen from Fig. 6, whereas with long fiber (LF) the porosity increased from 8.6 to 12.3% with increasing fiber content. The high value of porosity with increase in steel fiber content may be due to the tendency of the particles to clump together while mixing, entrapping water filled spaces, which consequently turn into voids. Increased fiber volume enhances the potential for fiber bailing and clumping. The slight increase in the porosity of specimens reinforced with steel fibers compared to the plain concrete can be explained by the fact that reinforced concrete specimens needed a long



(a)



(b)

Fig. 8 Sorptivity of SFRC with long fiber (a) small fiber; (b) long fiber

duration of vibration, which can affect the pores sizes and distribution.

Relation between specific porosity of SFRC and its electrical resistivity was investigated and plotted in Fig. 7. a-b depending on frequency for SF and LF containing SFRC. It is clear that the electrical resistivity decreases with an increase of porosity of SFRC at dried and saturated conditions. The electrical resistivity depends on the concrete's pores microstructure. All the changes of those properties, which result in changes in size and distribution of the concrete's pores, together with the variation of its humidity content and the curing conditions to which it is subjected, among others, affect the concrete's electrical resistivity. With the increase in the concrete's moisture content, the electrical resistivity decreases because the higher the humidity, the higher the quantity of the pores solution, making ionic mobility easier and consequently decreasing electrical resistivity.

Sorptivity measurement was carried out on SFRC and the results are presented in Fig. 8(a) and Fig. 8(b) for SFRC containing the SF and LF, respectively. The results indicate that the sorptivity of concrete increased uniformly with the increase in fiber content for both types of fiber. Generally, the capillary sorptivity of SFRC was higher than that of concrete without fibers for each group. When fiber length was considered regardless of fiber volume, it was observed that the sorptivity of SFRC decreased by fiber length increases. The water sorptivity tests results can be explained

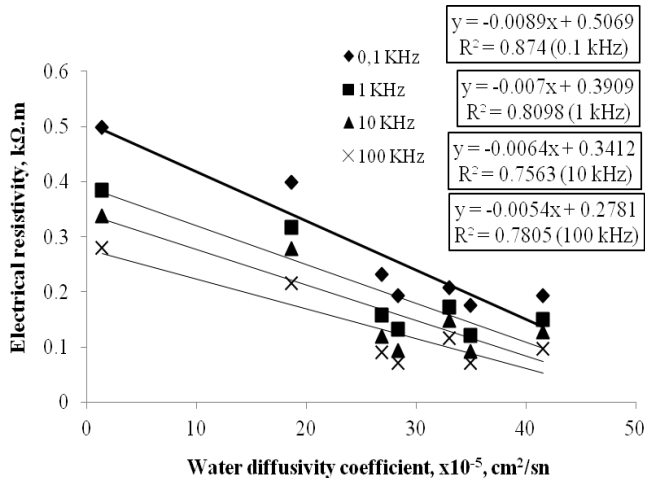


Fig. 9 Relation between diffusivity and electrical resistivity

by the fact that the presence of fibers, whatever their length or their content facilitated the interconnection between pores which were increased according to the porosity results. To explain such increase in the water sorptivity of SFRC, it may be assumed that capillarity is determined more by matrix properties than the fibers. In particular, the matrix-fiber interface has the largest content of pores and micro cracks that effect overall capillarity. The fiber acted as a bridge between pores so that the sorptivity was increased and the water sorptivity was subsequently also increased. Also, it is very important to mention here that SF higher act as ties between pores than LF so that interconnections are created which allow water to penetrate more easily inside the concrete structure (Atiş and Karahan 2009). The conductivity in concrete is also due to the presence of water in the capillary pores, which contains dissolved salts and acts as an electrolyte.

Electrical property measurements, as applied to cementitious materials, represent an additional and still developing investigative technique in the study of these materials both at the micro- and macro- scale. From an engineering point of view, there is a need to be able to characterize the capillary pore network using easily measured properties and, to this end, electrical measurements could be exploited. The electrical resistivity is a property which characterizes the higher or lower difficulty of the ions to move in the concrete's core, that is, it controls the ion flux in aqueous solution in the concrete's pores by diffusivity. Fig. 9 shows the changing of electrical resistivity of SFRC depending on water diffusivity. The diffusivity of hardened concretes depend upon the pore structure although in different ways. With the increase in the concrete's diffusivity coefficient, the electrical resistivity decreases because the higher humidity, the higher quantity of the pores solution, making ionic mobility easier and consequently decreasing electrical resistivity.

The relationship between the lateral carbonation depth of specimen and steel fiber content is shown in Figure 10. When the steel fiber content is 0-1.3%, with the increase of steel fiber, the concrete carbonation depth was gradually increased. When the mixing amount of steel fiber was increased, the contact between steel fiber and matrix

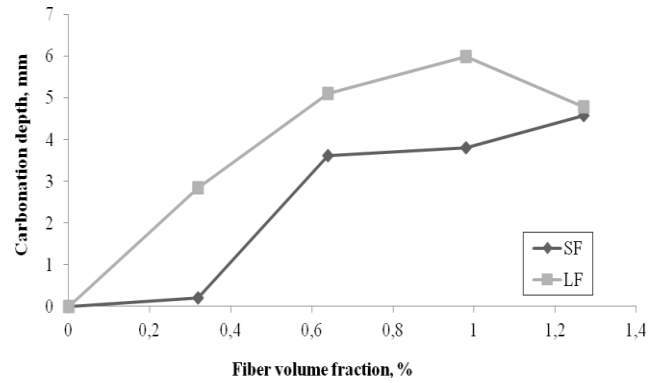


Fig. 10 Carbonation depth of SFRC depending on fiber content

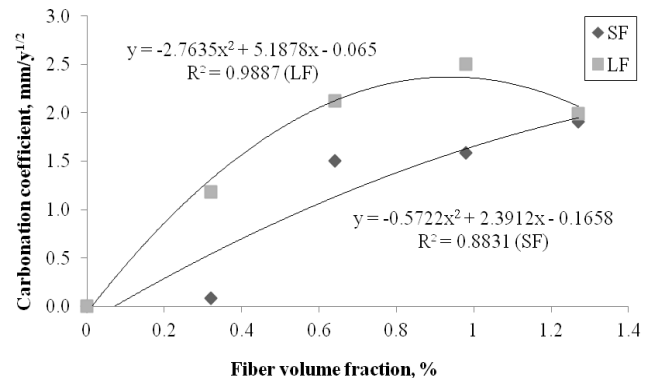


Fig. 11 Carbonation coefficient of SFRC depending on fiber content

concrete forms more weak binding interfaces, which makes CO<sub>2</sub> easy to spread in the concrete and increases the concrete carbonation depth.

The steel fibers increased carbonation coefficient of concrete (Fig. 11). To explain such increase in the carbonation coefficient of SFRC, it may be assumed that carbonation is determined more by matrix properties than the fibers. In particular, the matrix-fiber interface has the largest content of pores and micro cracks that effect overall carbonation. Also, it is very important to mention here that fibers act as ties between pores so that interconnections are created which allow CO<sub>2</sub> flow to penetrate more easily inside the concrete structure via capillary pores by diffusivity. The relation between carbonation coefficient and diffusivity ( $R=0.87$ ) that is given in Fig. 12 shows this phenomenon clearly. Carbonation reduces pH value and destroys the passive film around the steel (Yoon *et al.* 2015). The presence of even a small amount of chloride in carbonated concrete enhances the corrosion rate resulted from carbonation of concrete.

#### 4. Conclusions

Electrical resistivity measurement shows promise as a quality control and performance assessment tool for concrete materials. In this study, AC current at different frequency values has been applied to the hardened steel

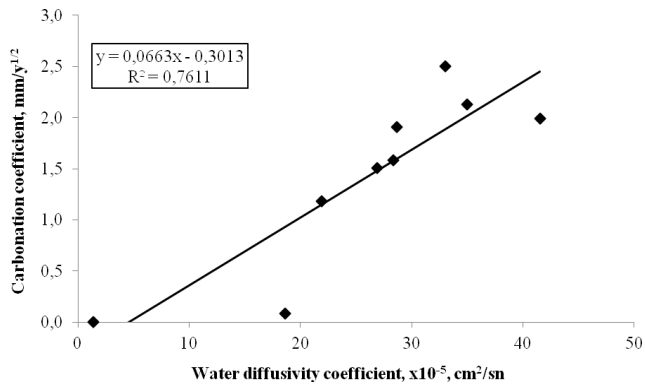


Fig. 12 Carbonation of concrete depending on diffusivity

fiber reinforced concretes which were produced by adding long and short fibers. The corrosion risk assessment were also performed on the SFRC by electrical resistivity method. The results which were obtained by this research study are given below:

Steel fiber addition to concrete clearly increases water capillarity and diffusivity coefficient whatever the fiber amount. This increase is also observed with specific porosity. The fibers acted as bridges between pores so that the water penetration was increased and water capillarity coefficients were subsequently increased. The fibers act as ties between pores so that interconnections are created which allow  $\text{CO}_2$  flow to penetrate more easily inside the concrete structure via capillary pores by diffusivity. As result of flowing of  $\text{CO}_2$  inside of SFRC, carbonation was increased by fiber content. It was observed that under extreme conditions, conductive steel fibers throughout the concrete volume, the reduction of the electrical resistivity caused by conductive fibers lead to a remarkable increase in the corrosion rate. However it is stressed that the case of corroding steel fibers throughout the concrete volume is due to the very high corrosion-resistance of embedded steel fibers. The highest values of electrical resistivity have been observed at the specimens without fibers since they have the lowest electrical current conduction. Electrical resistivity decreases with the use of fiber in concrete. Electrical resistivity also decreases when the percentage of fiber increases in concrete. Therefore, SFRC must be taken under protection against extreme conditions due to corrosion risk. Degree of corrosion can be measured by electrical current application. More corrosion has been observed at the specimens with long fibers than the specimens with short fibers. When the proportion of fiber has been increased both at the short and at the long fibers, the risk degree of corrosion has been increased. In conclusion, a connection between electrical resistivity and corrosion risk degree may be established through the application of different frequency ranges to the concrete. Both the use of long fibers and the increase of the strength of current at the concrete have enhanced the risk of corrosion, significantly. Corrosion of reinforcement, especially in the coastal infrastructure and road pavement applications with SFRC, is the major durability problem. The rate of corrosion can be primarily determined by the resistivity, local and/or bulk, depending on the corrosion process. It is consequently of inherent

interest to know how the overall bulk resistivity of the concrete varies with fiber content and moisture content, and, in particular how it develops over time under field conditions.

## References

- ASTM (1760), Standard Test Method for Bulk Electrical Conductivity of Hardened Concrete, West Conshohocken, PA, ASTM.
- Atiş, C.D. and Karahan, O. (2009), "Properties of steel fiber reinforced fly ash concrete", *Constr. Build. Mater.*, **23**(1) 392-399.
- Bertolini, L., Elsener, B., Pedferri, P. and Polder, R. (2004), *Corrosion of Steel in Concrete*, WILEY-VCH.
- Bouny, V.B., Kinomura, K., Thiery, M. and Moscardelli, S. (2011), "Easy assessment of durability indicators for service life prediction or quality control of concretes with high volumes of supplementary cementitious materials", *Cement Concrete Compos.*, **33**(8), 832-847.
- EN 197-1/A1 (2005), Cement, Part 1: Compositions and Conformity Criteria for Common Cements, Ankara, Turkey.
- Faifer, M., Ottoboni, R., Toscani, S. and Ferrara, L. (2011), "Nondestructive testing of steel-fiber-reinforced concrete using a magnetic approach", *IEEE Tran. Instrum. Measur.*, **60**(5), 1709-1717.
- Gjörv, O.E. (2013), "Durability design and quality assurance of concrete structures in severe environments", *Proceedings of the Seventh International Conference on Concrete under Severe Conditions - Environment and Loading*, Nanjing.
- Gu, P., Xie, P. and Beaudoin, J.J. (1993), "Impedance characterization of microcracking behaviour in fibre-reinforced cement composites", *Cement Concrete Compos.*, **15**, 173-80.
- Hallaji, M. and Ghaz, P.M. (2014), "A new sensing skin for qualitative damage detection in concrete elements: Rapid difference imaging with electrical resistance tomography", *NDT&E Int.*, **68**, 13-21.
- Hanžič, L. and Ilić, R. (2003), "Relationship between liquid sorptivity and capillarity in concrete", *Cement Concrete Res.*, **33**(9), 1385-1388.
- Hornbostel, K., Larsen, C.K. and Geiker, M.R. (2013), "Relationship between concrete resistivity and corrosion rate - A literature review", *Cement Concrete Compos.*, **39**, 60-72.
- Koleva, D.A., Copuroglu, O., Breugel, K.V., Yea, G. and Wit, J.H.W.D. (2008), "Electrical resistivity and microstructural properties of concrete materials in conditions of current flow", *Cement Concrete Compos.*, **30**, 731-744.
- Kyung, J.W., Tae, S.H., Lee, H.S., Alver, Y. and Yoo, J.H. (2007), "IBEM analyses on half-cell potential measurement for NDE of rebar corrosion", *Comput. Concrete*, **4**(4), 285-298.
- McCarter, W.J., Chrisp, T.M., Starrs, G. and Blewett, J. (2000), "Electrical conductivity, diffusion and permeability of Portland cement-based mortars", *Cement Concrete Res.*, **30**(9), 1395-1400.
- Michel, A., Solgaard, A.O.S., Geiker, M.R., Stang, H. and Olesen, J.F. (2009), "Influence of resistivity on the corrosion of reinforcement in concrete", *Proceedings of 3rd International PhD Workshop on Modelling the Durability of Reinforced Concrete*, Guimaraes.
- Monteiroa, A.O., Cachima, P.B. and Costab, P.M.F.J. (2015), "Electrical properties of cement-based composites containing carbon black particles", *Mater. Today: Proc.*, **2**, 193-199.
- Moris, W., Vico, A., Vazquez, M. and de Sanchez, S.R. (2002), "Corrosion of reinforcing steel evaluated by means of concrete resistivity measurements", *Corr. Sci.*, **44**(1), 81-99.

- Neithalath, N., Persun, J. and Ram, K. (2010), "Manchiryal Electrical conductivity based microstructure and strength prediction of plain and modified concretes", *Int. J. Adv. Eng. Sci. Appl. Math.*, **2**(3), 83-94.
- Oelsner, W., Berthold, F. and Guth, U. (2006), "The iR drop-well-known but often underestimated in electrochemical polarization measurements and corrosion testing", *Mater. Corros.*, **57**(6), 45-66.
- Pacheco, J., Šavija, B., Schlangen, E. and Polder, R.B. (2014), "Assessment of cracks in reinforced concrete by means of electrical resistance and image analysis", *Constr. Build. Mater.*, **65**, 417-426.
- Peled, A., Torrents, J.M., Mason, T.O., Shah, S.P. and Garboczi, E.J. (2001), "Electrical impedance spectra to monitor damage during tensile loading of cement composites", *ACI Mater. J.*, **98**, 313-322.
- Perumal, R. (2014), "Performance and modeling of high-performance steel fiber reinforced concrete under impact loads", *Comput. Concrete*, **13**(2), 255-270.
- Polder, R., Andrade, C., Elsener, B., Vennesland, Ø., Gulikers, J., Weidert, R. and Raupach, M. (2000), "Test methods for on site measurement of resistivity of concrete", *Mater. Struct.*, **33**(12), 603-611.
- Polder, R.B. (2001), "Test methods for on site measurement of resistivity of concrete-a RILEM TC-154 technical recommendation", *Constr. Build. Mater.*, **15**, 125-131.
- RILEM CPC-18 (1998), "Measurement of hardened concrete carbonation depth", *Materials and Structures, Research and Testing*, 435-440.
- Salbei, V.J., Sitters, C.M.W. and Vantomme, J. (2014), "Non-destructive testing techniques for corrosion assessment in reinforced concrete structures in Kenya", *Civil Environ. Res.*, **6**(7), 60-74.
- Şengül, Ö. (2014), "Use of electrical resistivity as an indicator for durability", *Constr. Build. Mater.*, **73**, 434-441.
- Solgaard, A.O.S., Carsana, M., Geiker, M.R., Küter, A. and Bertolini, L. (2013), "Experimental observations of stray current effects on steel fibres embedded in mortar", *Corr. Sci.*, **74**, 1-12.
- Tasdemir, C. (2003), "Combined effects of mineral admixtures and curing conditions on the sorptivity coefficient of concrete", *Cement Concrete Res.*, **33**(10), 1637-1642.
- Uygunoglu, T. (2011), "Effect of fiber type and content on bleeding of steel fiber reinforced concrete", *Constr. Build. Mater.*, **25**(2), 766-772.
- Wen, S. and Chung, D.D.L. (2000), "Damage monitoring of cement paste by electrical resistance measurement", *Cement Concrete Res.*, **30**, 1979-1982.
- Xiao, L. and Li, Z. (2008), "Early-age hydration of fresh concrete monitored by non-contact electrical resistivity measurement", *Cement Concrete Res.*, **38**, 312-319.
- Yoon, I.S., Hong, S. and Kang, T.H.K. (2015), "Influence of curing condition and carbonation on electrical resistivity of concrete", *Comput. Concrete*, **15**(6), 973-987.
- Yury, A., Zaccardi, V., Angel, A. and Maio, D. (2014), "Electrical resistivity measurement of unsaturated concrete samples", *Mag. Concrete Res.*, **66**(10), 484-491.